

# *Image Reconstruction of Tang Sancai Figurines Based on Artificial Intelligence Image Extraction Technology Based on Ration*

Shengwei Qiu\*

*Department of Information Engineering, Heilongjiang International University, Heilongjiang, China*

*qiushengwei@hiu.net.cn*

*\*corresponding author*

**Keywords:** Artificial Intelligence Algorithm, Image Extraction Technology, Image Reconstruction, Tang Sancai Figurines

**Abstract:** In the process of studying the Tang Sancai figurines, some images will be degraded due to optical system, motion, atmospheric turbulence, etc., so the images need to be restored. With the best restoration method, the restored image can meet the requirements. In fact, the purpose of image restoration is to process the degraded image to make the restored image closer to the original image. This paper conducts a comparative experiment on the classical image reconstruction methods, taking the images of Tang Sancai figurines as the experimental objects. The results show that the image reconstruction quality of the least squares method is the best among the methods selected for the experiment in this paper, and the SSIM and PSNR index values of the reconstructed image A are 0.9612 and 31.7612, respectively; in the performance comparison of GAN, GA-GAN, and Dense-GAN models, the image reconstruction algorithm based on the GA-GAN model has the best performance. Among the ten images of Tang Sancai figurines used in the experiment, the highest SIMM value is 0.99, and the highest PSNR value is 27.9345.

## 1. Introduction

Humans mainly acquire important information through vision, and images are one of the important sources of visual information. However, in the living environment, we will encounter many unexpected events and factors that are beyond our control, resulting in the degradation of the

quality of image generation, storage and transmission, seriously affecting the image quality of photos. The deterioration of image quality is mainly caused by the following reasons: Gaussian blur, motion blur, a certain degree of image distortion, etc. This process is called image degradation. If the image is degraded, the image cannot be recognized. Research on image restoration methods is of great value, and all aspects of society require high-quality images. Therefore, the research on image restoration objects is of great significance.

Computer vision is an indispensable key technology in daily life and production. Whether in daily life or in industrial production, it is the main way to obtain visual information and is very important for obtaining high-quality images. Due to a series of reasons such as outdated hardware system or harsh environment, it often brings great interference to image acquisition, resulting in inability to obtain high-quality images. While image quality can be improved by improving iterative hardware, the cost of image acquisition can be greatly increased. Several image reconstruction methods proposed in this paper provide new reference directions for image restoration and inject new blood into the development of image restoration.

The continuous development of artificial intelligence technology provides important technical support for image reconstruction. The innovations of this paper are: First, various traditional image reconstruction algorithms are compared and improved; the second is to compare the performance of image reconstruction models based on artificial intelligence image extraction technology; the third is to improve the image reconstruction algorithm based on the GAN model, and the performance is compared; the fourth is to set up an image dataset of Tang Sancai figurines.

## 2. Related Work

In real-world image processing, a lot of prior knowledge is unknown. Obtaining prior knowledge of images is very difficult, and in some cases impossible. Finding reliable and practical image restoration methods has always been a concern of researchers. In recent years, many new methods have been proposed in various fields. Zhang J has conducted in-depth research and exploration on the principles and methods of image edge extraction. First, he analyzed and discussed the meaning and prospect of image edge extraction, then introduced the basic theory of image extraction, enumerated and explained various current extraction algorithms, and focused on the canny algorithm and robot algorithm. And through experimental simulation, he obtained the respective extracted images from the aspects of image extraction effect, peak signal-to-noise ratio and time overhead [1]. On the basis of image processing and recognition theory, and combined with improved ticket information recognition technology, Hu S proposed a ticket number recognition data collection and recognition algorithm based on improved BP neural network, and used the tilt detection method based on the Bresenham integer algorithm to correct the tilted bill image [2]. Technological advancements in artificial intelligence and machine learning have the potential to profoundly impact how DNLE systems operate, and in turn, content creation methods will change dramatically. Ohanian T studies the impact of image recognition, natural speech processing, language recognition, cognitive metadata extraction, pitch analysis, and data and statistical integration on content creation [3]. Bhargavi VR uses a publicly available database for demonstrating the implemented strategy, applying a support vector machine classifier to evaluate the performance of the applied technique in terms of sensitivity, specificity and accuracy. Compared with other eigenvectors, his implemented LE-based eigenvectors have better classification performance, with SIFT-LE-SVM achieving 96.6% accuracy [4]. Wang X employs a manifold learning algorithm for dimensionality reduction on grayscale and RGB color images. In his experiments he applied three clustering algorithms to achieve sharper images. Locally, Linear Embedding (LLE) and Gustafson–Kessel (GK) algorithms are used to extract image features. The

results show that the recognition rates of feature extraction for grayscale images and color images are 95% and 99%, respectively [5]. Gupta H proposes a new image reconstruction method that replaces the projector in projected gradient descent (PGD) with a convolutional neural network (CNN). Unlike existing iterative image reconstruction algorithms, these CNN-based methods often lack feedback mechanisms to enforce that the reconstructed images are consistent with the measurements. The CNN recursively projects the solution to a space closer to the desired reconstructed image [6].

### 3. Method of Image Reconstruction of Tang Sancai Figurines Based on Artificial Intelligence Image Extraction Technology Based on Ration

#### 3.1. Overview of Image Reconstruction Technology

##### (1) Image degradation model

In the research of image restoration and reconstruction, due to the imperfect imaging system equipment and transmission medium, the equipment and the object cannot be absolutely static, and the interference mixed in the imaging process, the original quality of the image will be degraded, so the primary task of conducting research is to establish a linear mathematical model of image degradation, which is shown in Figure 1.

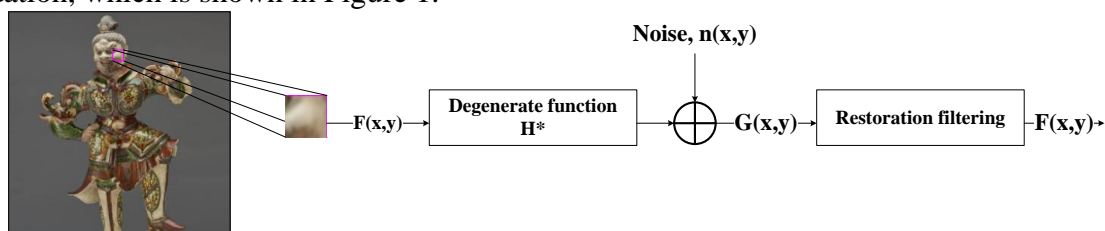


Figure 1. Image degradation linear model

The linear process in Figure 1 can be expressed as:

$$G(x,y) = H[F(x,y)] + n(x,y) \tag{1}$$

By discretizing equation (1), we get:

$$G(x,y) = \sum_r \sum_t H(r,t)F(x-r,y-t) + n(x,y) \quad (x = 1,2, \dots, M; y = 1,2, \dots, N) \tag{2}$$

In order to improve image quality after image degradation, inpainting and enhancement are necessary. The SR image technique, by means of a digital processor, complements the lost detailed information, allowing the conversion of the lost low-resolution images into more informative high-resolution images [7-8]. As shown in Figure 2, the resulting image after ultra-precise processing has sharper textures, softer edges, and more clearly visible.

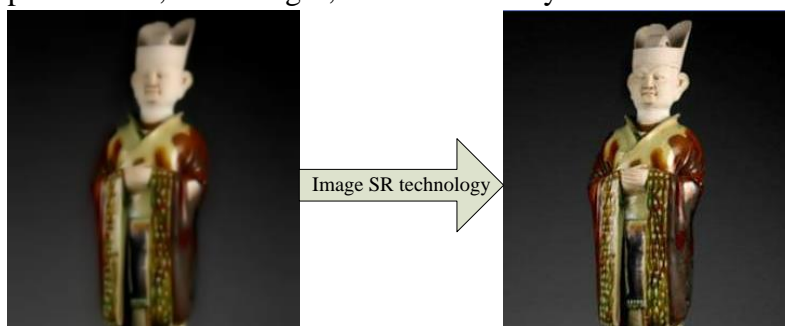


Figure 2. Resolved reconstruction contrast

## (2) Image restoration method

The core of image restoration is to make the restored image closer to the original image through prior knowledge, such as degraded image  $G$ , degraded model  $H$  and noise  $n$ . Since most recovery methods have their own limitations, they are not widely used in practice. This section briefly summarizes some traditional computational methods [9-10].

### 1) Minimal Squares Image Restoration

Least squares image restoration is an image restoration method with constraints, also known as regularized filter restoration. For such extreme value problems with constraints, the Lagrange multiplier method can be used to solve:

$$K(\hat{F}) = \|P\hat{F}\|^2 + \alpha \left[ \|G - H\hat{F}\|^2 - \|n\|^2 \right] \quad (3)$$

$$\|G - H\hat{F}\|^2 = \|n\|^2 \quad (4)$$

Letting  $P$  be the  $F$  linear operator, so the image reconstruction can be converted into a function related to  $\|P\hat{F}\|^2$ , formula (4) is the constraint condition of the function,  $\alpha$  is the Lagrangian number, and through the change of the  $P$  value, different targets can be restored, perform partial differentiation on  $\hat{F}$  to get formula (5), and  $\beta$  is a constant.

$$\hat{F} = (H^T H + \beta P^T P)^{-1} \quad (5)$$

$$\beta = \frac{1}{\alpha} \quad (6)$$

### 2) Blind deconvolution restoration

There are many methods for blind deconvolution restoration. This article mainly introduces the Richardson-Lucy algorithm, which is evolved from the Bayesian formula.

$$P(x|y) = \frac{P(y|x)P(x)}{\int P(y|x)P(x)dx} \quad (7)$$

Combining this with the degenerate model to get the iterative function:

$$F_{i+1}(x) = \int \frac{G(y,x)P(y)dy}{\int G(y,z)F_i(z)dx} F_i(x) \quad (8)$$

$F_i(x)$  is the  $i$ -th round of iterative restoration of the image,  $G$  and  $P$  are degradation functions, and assume that the blur functions in each area of the image are consistent, and the iterative formula is further changed to:

$$F_{i+1}(x) = \left\{ \left[ \frac{P(x)}{F_i(x) \otimes G(x)} \right] \otimes G(-x) \right\} F_i(x) \quad (9)$$

$F_i(x)$  represents the reconstructed image in the  $k$ th round. The iterative solution only needs to know the initial estimate  $F_0(x)$  when the degradation function PSF is known, and then the final  $G(x)$  and  $F(x)$  can be obtained by continuous iteration.

$$G_{i+1}^k(x) = \left\{ \left[ \frac{P(x)}{G_i^k(x) \otimes F^{k+1}(x)} \right] \otimes F^{k-1}(-x) \right\} G_i^k(x) \quad (10)$$

$$F_{i+1}^k(x) = \left\{ \left[ \frac{P(x)}{F_i^k(x) \otimes G^k(x)} \right] \otimes G^k(-x) \right\} F_i^k(x) \quad (11)$$

### 3) Maximum entropy restoration

The total energy of the image is:

$$E_{\text{Sum}} = \sum_x \sum_y F(x,y) \quad (12)$$

The entropy value is:

$$e_F = -\sum_x \sum_y F(x,y) \ln F(x,y) \quad (13)$$

The noise entropy is:

$$e_N = -\sum_x \sum_y (N(x,y) + D) \ln [N(x,y) + D] \quad (14)$$

D is the minimum negative noise value, assuming  $0 \ln 0 = 0$ , satisfying the constraints of the image degradation model and formula (12), the image entropy and noise entropy of the restored image can be maximized. By defining various forms of entropy, different recovery methods are thus formed.

### 3.2. Image Reconstruction Algorithm Evaluation Method

The quality of image reconstruction is divided into subjective evaluation and objective evaluation. Subjective evaluation is to evaluate the quality of the image through human feeling, and objective evaluation is to evaluate the quality of the image through some quantitative indicators. People still have certain limitations on visual analysis research, and usually combine subjective perception and objective criteria to consider the quality of the image [11-12].

#### (1) Subjective evaluation

Subjective evaluation usually evaluates image quality from the perspective of subjective visual perception. Differences in different types of images and observed environments, interests of different evaluators, personal preferences, etc., will lead to different results. Subjective evaluation uses the visual system of the observer to directly make subjective judgments on the changes before and after the image. The average opinion score method is a commonly used method for evaluating images, which is mainly divided into absolute evaluation and relative evaluation [13-14].

Absolute evaluation is the sensory judgment of the original image and the reconstructed image by the evaluator according to their own preferences. The relevant standards are shown in Table 1.

Table 1. Subjective absolute evaluation scale criteria

Absolute evaluation quality scale		Absolute evaluation obstacle scale	
5	No degradation of image quality can be seen at all.	5	Very good
4	Slight degradation of image quality can be seen.	4	Good
3	Clearly see the degradation of image quality.	3	Common
2	Have an obstacle to viewing.	2	Be poor
1	Very serious obstruction to viewing.	1	Very poor

In the relative evaluation method, the evaluator observes a series of SR images uniformly, and scores the effect of each reconstructed image, as shown in Table 2.

Table 2. Relative evaluation scale criteria

Mark	Relative evaluation scale	Absolute evaluation index
5	The best level in the group	Very good
4	Better than the average level in the population.	Good
3	Average level in population	Common
2	The worst level in a group	Be poor
1	The best level in the group	Very poor

It is worth noting that no matter which method is used, an intuitive, direct and subjective

evaluation is made through one's own judgment. In order to ensure the rationality and accuracy of the evaluation results, it should be ensured that enough observers participate in the evaluation, so that the evaluation results are closer to the actual situation. The use of group evaluation methods is of great significance for image evaluation.

(2) Objective evaluation

The peak signal-to-noise ratio is mainly to evaluate the quality of the image by calculating the error between the corresponding pixel positions of the two images. Letting the number of bits per pixel be  $n$ , and MSE represents the mean square error of  $X$  and  $Y$ ;  $H$  is the image height and  $W$  is the width;  $X(i,j)$  and  $Y(i,j)$  represent the pixel values at the image position.

$$MSE = \frac{\sum_{i=1}^H \sum_{j=1}^W [X(i,j) - Y(i,j)]^2}{H \cdot W} \quad (15)$$

$$PSNR = 10 \log_{10} \frac{(2^n - 1)^2}{MSE} \quad (16)$$

Structural similarity is mainly used to measure the similarity between images, and it will measure the degree of image distortion from three aspects: brightness, contrast and structure. SSIM satisfies symmetry and validity, using the mean of pixels to estimate the brightness of the image, the variance of the pixels to estimate the contrast, and the covariance of the pixels to estimate the similarity of the image structure [15].  $B$ ,  $C$  and  $S$  represent brightness, contrast and structure functions, respectively,  $\mu$  is the image mean,  $\sigma$  is the variance,  $\sigma_{XY}$  is the covariance of the image, and  $M_1$ ,  $M_2$ , and  $M_3$  are constants.

$$B(X, Y) = \frac{2\mu_X\mu_Y + M_1}{\mu_X^2 + \mu_Y^2 + M_1} \quad (17)$$

$$C(X, Y) = \frac{2\sigma_X\sigma_Y + M_2}{\sigma_X^2 + \sigma_Y^2 + M_2} \quad (18)$$

$$S(X, Y) = \frac{\sigma_{XY} + M_3}{\sigma_X\sigma_Y + M_3} \quad (19)$$

$$SSIM = B(X, Y) * C(X, Y) * S(X, Y) \quad (20)$$

The RGB color distance method is also a qualitative image evaluation method, which is an algorithm based on natural light. In a digital image, each color with different shades can be represented by RGB values of different sizes, as shown in Figure 3, the value range of R, G, and B is [0, 255].

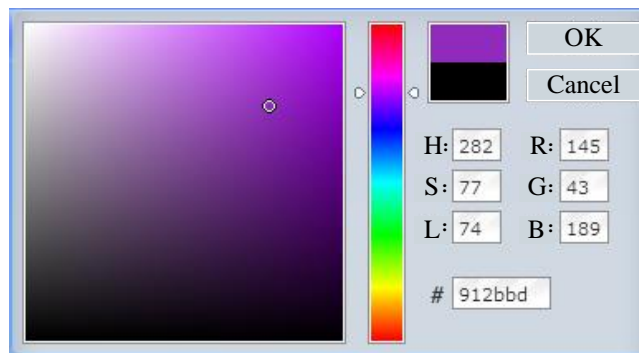


Figure 3. Color numerical representation

Generally, any point value is expressed as a three-dimensional vector, and the chromatic aberration difference of the comparison images is quantitatively expressed by the chromatic spatial



distance of the same position of the two images. When the value of the distance  $L$  is smaller, it indicates that the color difference between the two points is closer. The calculation method is:

$$L = \sqrt{(R_1 - R_2)^2 + (G_1 - G_2)^2 + (B_1 - B_2)^2} \quad (21)$$

### 3.3. Artificial Intelligence Image Extraction Technology

In order to allow computers to better recognize images, humans use bionics to introduce intelligent neural network algorithms to computers.

#### (1) Image extraction based on BP neural network

The structure of BP neural network is shown in Figure 4, which includes input layer, hidden layer and output layer. BP neural network algorithm simulates the processing and information transfer process of human neural network. The multi-layer feedforward neural network is trained by the error back propagation algorithm. The BP neural network is composed of a bidirectional learning process. The two direction signals are the forward signal and the reverse error signal respectively. The input signal first enters the input layer of the BP neural network from the outside, and then enters the middle layer of the BP neural network through the input layer. When the output signal cannot reach the predetermined output, it starts back-propagation and returns the error between the expected output and the actual output through the original route [16-17]. In the feedback process, the BP neural network can associate the weights of different levels to reduce the feedback error. If the above process cannot achieve the expected output, it iterates in the BP neural network, the final output signal will be lower than the expected value, and then the output signal is output through the output layer.

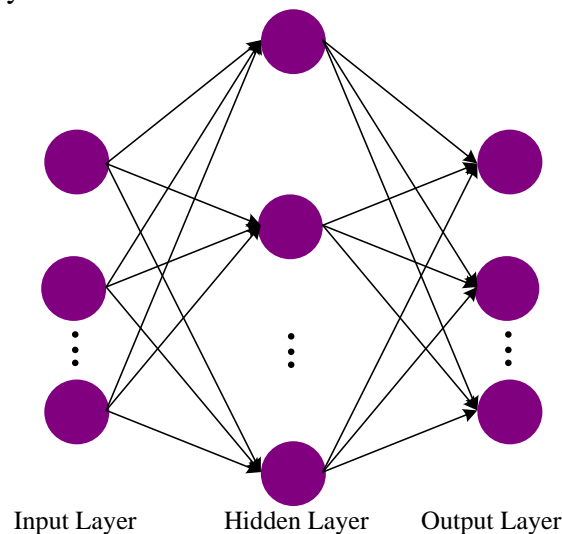


Figure 4. BP neural network structure

#### (2) Image extraction based on CNN network

CNN is a feedforward neural network based on artificial intelligence, at present, it has outstanding achievements in the fields of image recognition and processing, and super-resolution. The structure diagram of convolutional neural network is shown in Figure 5, which mainly includes input layer, hidden layer and output layer. Hidden layers include convolutional layers, pooling layers, and fully interconnected layers. In the hidden layer, convolution kernels are used to perform feature extraction on input random noise or low-resolution images, and then the relationship between objects is achieved through the interaction between different layers [18]. Low-level feature

convolutional layers are an important part of convolutional neural networks. It is controlled by three parameters: depth, step and fill value.

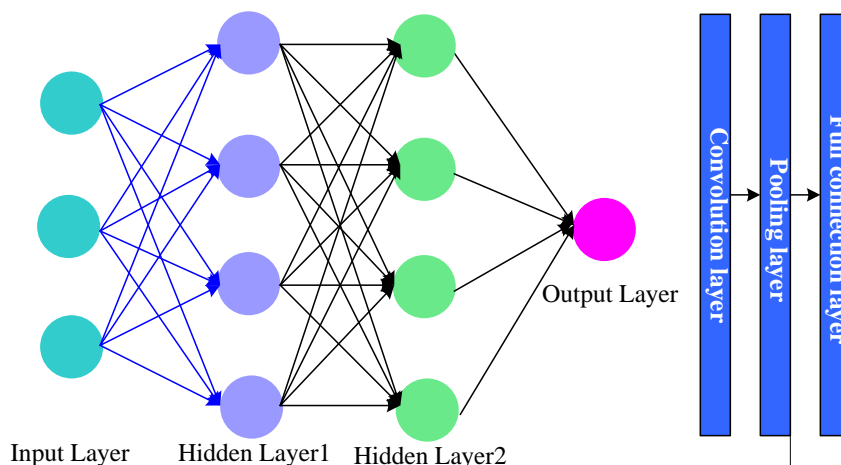


Figure 5. CNN network structure

Before performing the convolution operation on the image, it is necessary to fill the part with insufficient edges, and the image through the convolution operation will have more feature layers, so the feature information of adjacent areas is easy to repeat. Therefore, a pooling layer is introduced into the hidden layer, and the fully connected layer can play a role in distributed feature representation. The value of the current layer node is weighted and assigned to all the nodes in the previous layer.

(3) Image extraction based on GAN network

Generative adversarial network is a popular deep learning network framework. It is generally built with convolutional layers. The images generated by GAN can retain more texture details and are more realistic. Therefore, in many low-level visual tasks, it is often used. GAN learns the generative model of data distribution in a confrontational way. In image reconstruction, supervised learning is mainly used to learn the mapping relationship from blurred images to clear images. Its structure is shown in Figure 6. Its structure consists of a generator and a discriminator. Both the generator and the discriminator are neural networks. The generator uses the prior distribution  $Z$  to generate results close to the real samples. The discriminator is equivalent to a classifier, and the output value is a probability or probability matrix. The larger the probability value, the more real the input is [19-20].

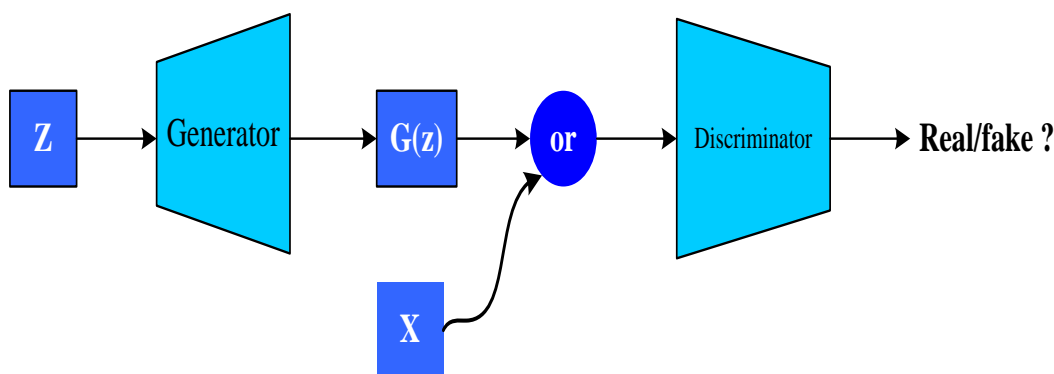


Figure 6. GAN structure



## 4. Image Reconstruction Experiment of Tang Sancai Figurines Based on Artificial Intelligence Image Extraction Technology Based on Ration

### 4.1. Experimental Results and Analysis of Classical Image Reconstruction Methods

In the experiment, the traditional image reconstruction method is firstly studied. On the basis of matlab2015, a Gaussian blur of  $9 \times 9$  and a variance of 1 is given to the image of A Tang tri-colored figurine. The image is restored by the three methods introduced in the paper, namely, the minimum square image restoration, the blind deconvolution restoration, and the maximum entropy restoration. The restoration results are shown in Figure 7. From (a) to (e) in the figure are the original image, Gaussian blur, least squares, maximum entropy restoration and blind deconvolution restoration respectively. It can be seen from the figure that the effects of least squares image restoration and maximum entropy restoration are both better than those of blind deconvolution restoration. Blind deconvolution restoration has problems such as darker pictures, more noise, and unclear figures. The effect of the least squares restoration method is relatively close to the original image, and the lines of the figures are clearer and the texture details are richer.

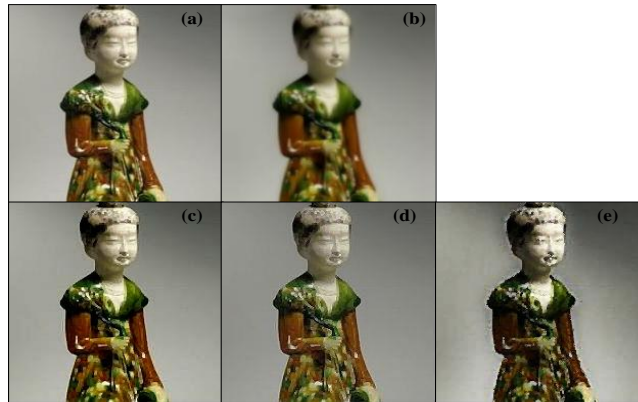


Figure 7. Traditional method image reconstruction

The image restoration effect is judged by using the peak signal-to-noise ratio and similarity as evaluation indicators. The restoration data of A image are shown in Table 3. It can be seen from the table that the least squares restoration method has the largest SSIM value and PSNR value among several traditional methods for restoring the image of Tang Sancai figurines A, indicating that the image reconstruction effect of this method is the best. The relevant index value of the blind deconvolution restoration method is the smallest, indicating that the reconstruction effect of this method is the worst.

Table 3. SSIM and PSNR of Image A reconstruction

Recovery method	SSIM	PSNR(dB)
Least square method	0.9612	31.7612
Maximum entropy	0.8463	26.2706
Blind deconvolution	0.7801	18.1054

In this study, another image B of Tang Sancai figurines was used for image reconstruction

experiments. The SSIM and PSNR values of the reconstructed images obtained by various methods are shown in Table 4. The results are the same as Figure A, the SSIM and PSNR values of the blind deconvolution image reconstruction method are the smallest, which still shows that the blind deconvolution reconstruction effect is the worst, the index value of the least squares method is the highest, and the image reconstruction effect is the best.

*Table 4. SSIM and PSNR of Image A reconstruction*

Recovery method	SSIM	PSNR(dB)
Least square method	0.9374	29.0216
Maximum entropy	0.8289	24.8372
Blind deconvolution	0.6953	15.5961

## 4.2. Experimental Results and Analysis of Image Reconstruction Method Based on Artificial Intelligence Image Extraction Technology

### (1) Experimental dataset

In this part of the experiments, the quality of the reconstructed images is qualitatively and quantitatively assessed using two sets of data. The first set of data is the GoPro dataset, which contains 3214 pairs of sharp images with a resolution of  $1280 \times 720$ . Blurred images are formed in the dataset by averaging short exposures of consecutive video frames. A high frame rate camera is used to form blurred frames around long exposure times, rather than nuclear blur composites. Of these data, 2103 pairs of network models were used to train the algorithm, and 1111 pairs of images were used to test the performance of the models. The model used in this chapter is a  $256 \times 256$  image patch obtained by randomly cropping 2103 images in the GoPro training set. The whole image is used to evaluate the blurring performance of the model.

The second data set is formed by collecting pictures related to Tang Sancai figurines in this paper. 156 clear and publicly available pictures of Tang Sancai figurines are downloaded from the Internet, and the images are cropped to a uniform size. The blurred images corresponding to these pictures are formed by Gaussian blurring and added noise, which can also be evaluated qualitatively and quantitatively. This paper will use this data set to test the effect of various artificial intelligence image extraction algorithms on the reconstruction of images of Tang Sancai figures.

### (2) Experimental results and performance analysis

Experiments are implemented using the Python programming language with the Pytorch deep learning framework. Using the GOPRO dataset to train several artificial intelligence learning models CNN, GAN and BP network models mentioned above, both the GAN generator and the discriminator model parameters are updated by the Adam optimizer, the optimizer parameters are set as: the first-order moment estimate exponential decay rate is 0.5, the second-order moment estimation exponential decay rate is 0.99, the number of training iterations is set to 2500, and the initial learning rate is set to 0.001. The final training result is shown in Figure 8. As can be seen from the figure, in the training experiment, the fastest training completion speed is the GAN model. When the number of iterations is about 1800, the image extraction and discrimination error rate is close to 0; the second is the CNN learning model, which has the lowest error rate when the number of iterations reaches about 2,100; the last is the image extraction model based on the BP neural network model, which has the lowest error rate when the number of iterations is 2,200. It can be

seen that the speed performance of the three models is not very different, and the performance of the GAN model is slightly better.

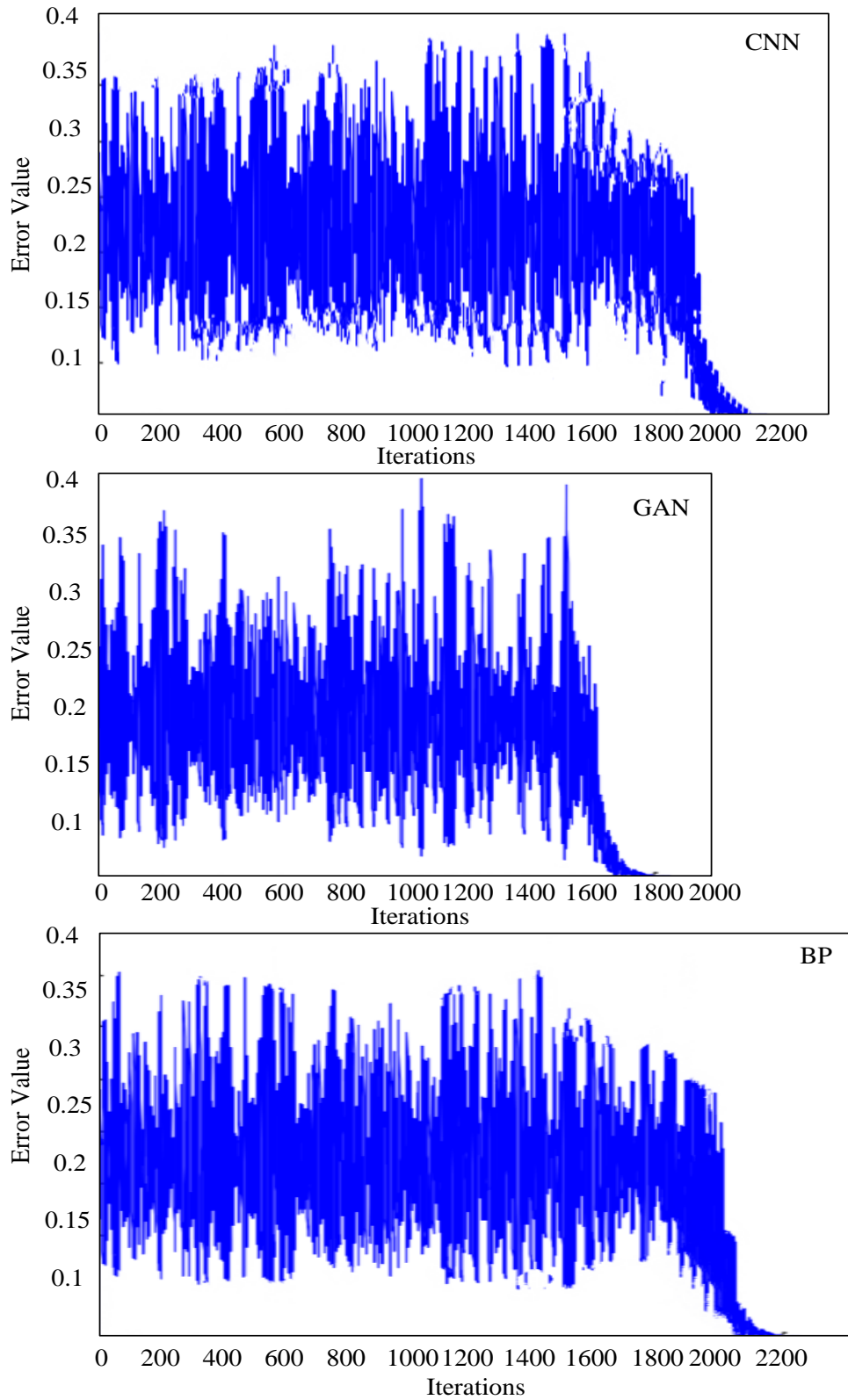


Figure 8. Each model training is completed

For the least squares image reconstruction method, the maximum entropy image reconstruction method, the image reconstruction algorithm based on BP neural network, the image reconstruction algorithm based on CNN, the image reconstruction algorithm based on GAN and the image reconstruction model based on GA-GAN on the GOPRO dataset Algorithms for comparative experiments, these algorithms are represented by the letters A-F respectively. The effect of image reconstruction is quantitatively and qualitatively analyzed, and the performance of the restoration algorithm is evaluated according to the detection results. The parameters in the model are updated by the Adma optimizer. The evaluation indicators used for quantitative evaluation are SSIM and PSNR, and the quantitative analysis results of each method are shown in Figure 9. In the experimental method, all deep learning algorithms are trained using the GOPRO dataset, it can be seen from the experimental results that relatively speaking, the reconstructed image quality under the image reconstruction method based on artificial intelligence image extraction technology is better. Among them, the improved GAN algorithm model, namely the GA-GAN algorithm, has the best image reconstruction performance, and its index values SSIM and PSNR are the highest among the tested methods, which are 0.96 and 29.82, respectively. The second is the GAN algorithm, whose SSIM value and PSNR value are 0.927 and 28.7, respectively. Among the traditional image reconstruction methods, the maximum entropy image reconstruction method has poor performance.

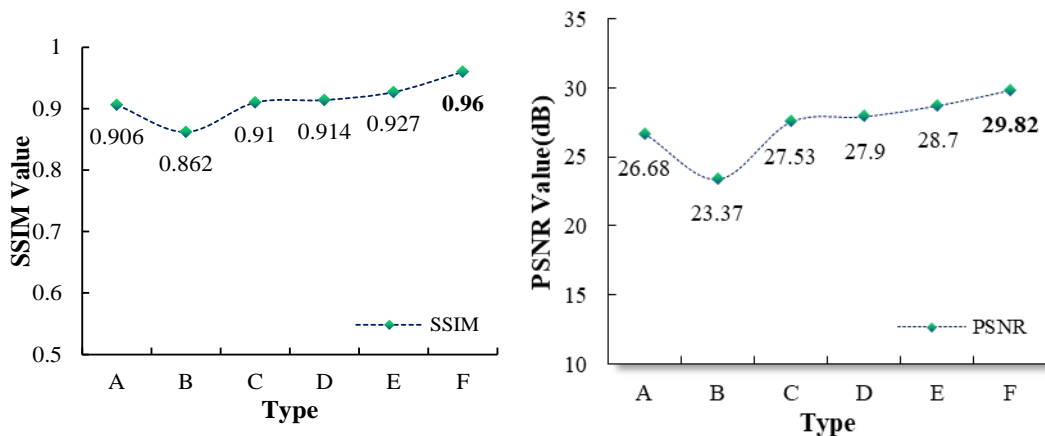


Figure 9. Quantitative comparison on the GOPRO dataset

The experiment is carried out using the self-built Tang Sancai figurine dataset. The compared models are the GAN-based image reconstruction algorithm, the Dense-GAN-based image reconstruction algorithm, and the GA-GAN-based image reconstruction model. The qualitative evaluation of image reconstruction technology was carried out first, and 10 observers were set up to use these models to restore and reconstruct 10 images of Tang Sancai figurines randomly selected from the data set. 10 observers were asked to rate the post-reconstruction image quality effect according to the relative evaluation criteria table. According to the average opinion score method, the average score of each observer on the reconstructed image effect of different models is calculated, and the results are shown in Figure 10. Since the relative evaluation standard table assigns 1-5 points according to the 1-5 level of the reconstructed image, judging from the average of the scores of the observers, the image reconstruction model based on the GA-GAN algorithm can visually restore the image of the Tang Sancai figurines to be better than the other two algorithm models.

Quantitative evaluation of the image reconstruction effect of each model was carried out, and 9 images of random Tang Sancai figures with Gaussian blur and noise were selected, and GAN, Dense-GAN, and GA-GAN image reconstruction models were used for image restoration. Each model is represented by A, B, and C, respectively. The restored image statistical index value SSIM

and PSNR value are used to objectively evaluate the model. The quantitative analysis results are shown in Figure 11. From the SSIM and PSNR output values in the figure, it can be seen that the three image reconstruction models of GAN, Dense-GAN and GA-GAN are based on GA-GAN generation confrontation, whether they are compared on the SSIM index value or the PSNR index value, the quality of the images of Tang Sancai figurines reconstructed by the network image reconstruction model is better, the second is the image reconstruction algorithm based on the Dense-GAN model, and the last is the GAN algorithm. This also shows that the performance of the improved GAN image reconstruction model is better than that of the unimproved GAN image reconstruction model. It can be proved that the connection method of the dense module to further closely fit the network layer can bring about the improvement of image super-resolution performance. However, the color of the image generated based on Dense-GAN appears to be saturated. The color of the image generated based on GA-GAN will be closer to the real image, and the picture will be more delicate and clear. From the perspective of visual sense, compared with the original blurred image, the restored image by each method is obviously clearer, but it is difficult to clearly distinguish the difference of the details of the image. Therefore, it is also necessary to evaluate the image in a local area. By comparing the image blocks cut out from each image, the pros and cons of each method can be judged.

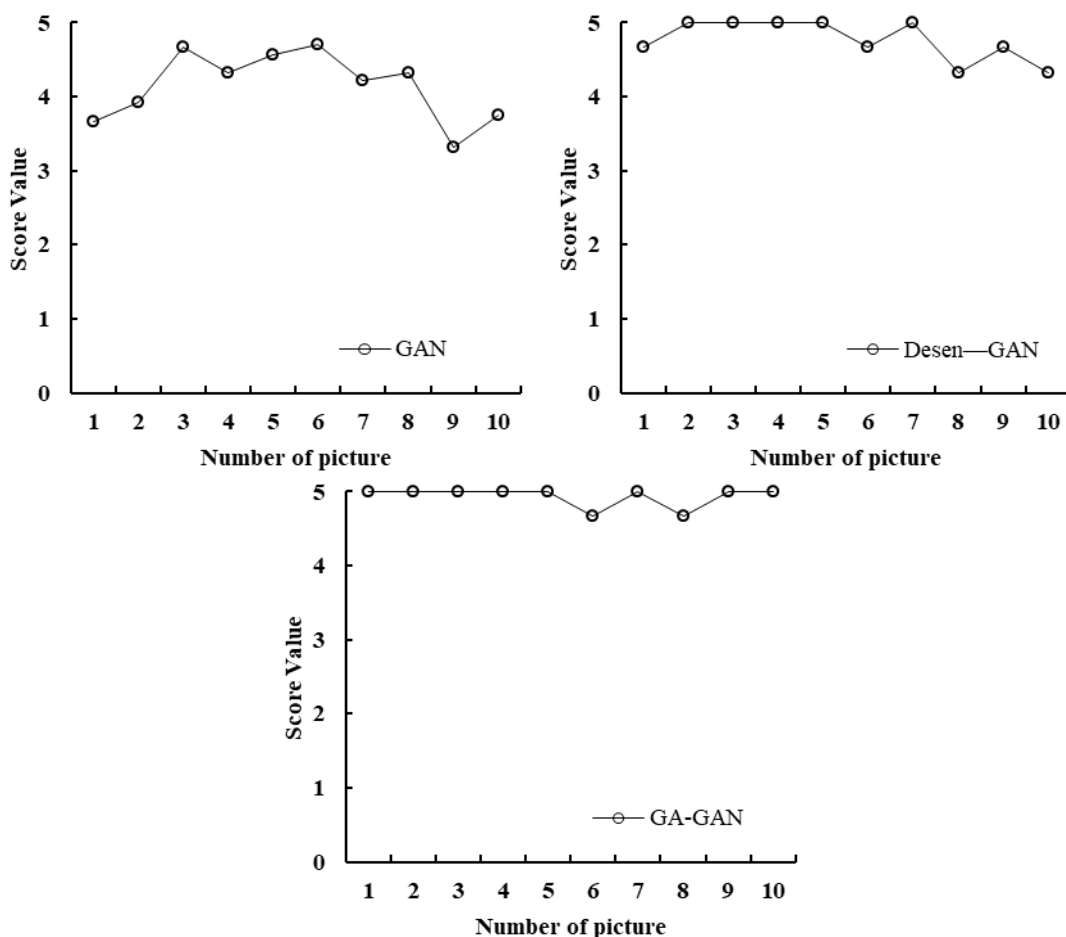


Figure 10. Mean opinion score

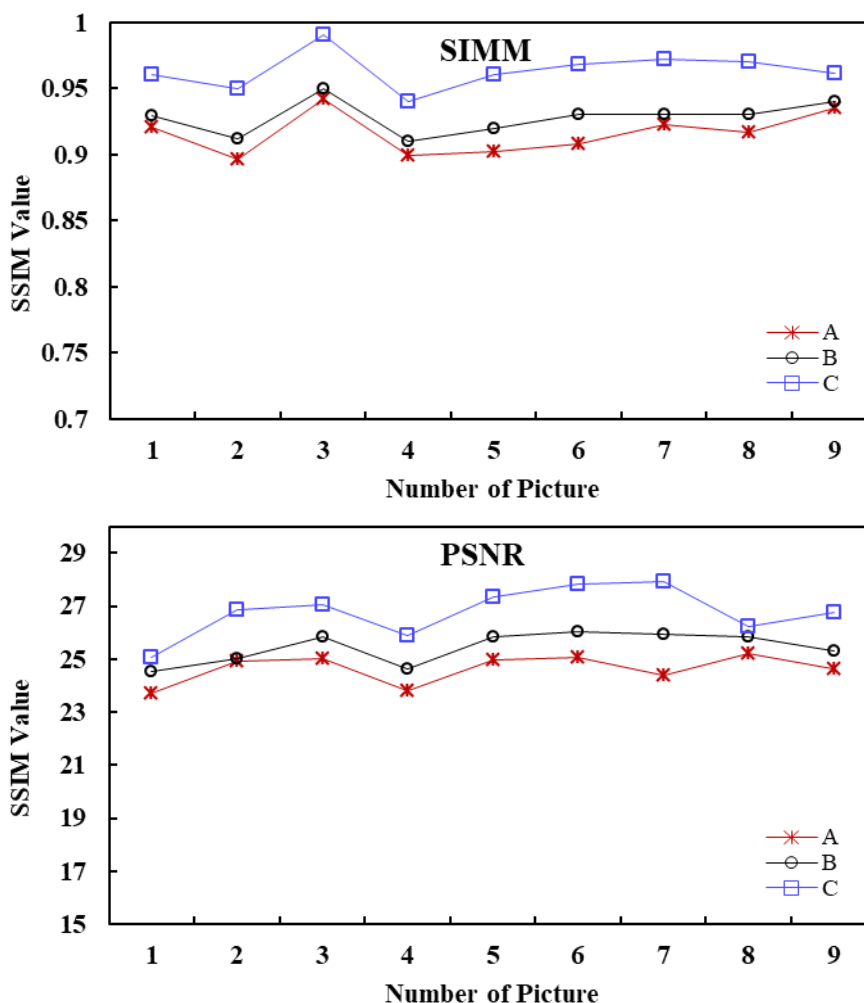


Figure 11. Objective evaluation of reconstructed image quality

## 5. Discussion

This paper is a research on the image reconstruction of Tang Sancai figurines based on Ration's artificial intelligence extraction technology. Image restoration is a research hotspot in the field of artificial intelligence applied to image processing. The first part of this paper introduces the relevant research background and research significance of image restoration, and refines the innovation of this paper. The second part of the article summarizes relevant research results and evaluates the research strengths of others. The third part of the article is an overview of related technologies and a summary of research methods. First, the image reconstruction technology is introduced, including the basic image degradation model in image reconstruction, image restoration methods, and image restoration methods. The article mentioned the least squares image restoration, blind area convolution restoration, maximum entropy restoration; secondly, the evaluation method of image reconstruction algorithm is summarized. The image reconstruction evaluation method is mainly divided into two parts, the subjective evaluation method and the objective evaluation method; then, the artificial intelligence extraction technology involved in the experimental research is summarized and outlined. There are mainly three deep learning methods, namely: Image feature extraction technology based on BP neural network, image feature extraction technology based on CNN convolutional neural network and image extraction technology based on GAN confrontation generation network. The fourth part of the article is the main experimental research and result



analysis part, which is divided into two subsections. The first section is an experimental comparative study of classical image reconstruction methods. The main methods are minimizing square image restoration, blind deconvolution restoration and maximum entropy restoration, the evaluation indicators used are SSIM value and PSNR value. The experimental results show that among these methods, the image quality of the image restored by the least squares method is the best. Whether it is from the visual perception or the quantitative evaluation index value, the least squares reconstructed images show the best reconstruction quality. The content of the second subsection is the experimental research on artificial intelligence image extraction technology. There are two types of data sets selected for the experiment, one is the GoPro data set, and the other is the Tang Sancai figurine data set built by me. Experimental research shows that among the image extraction technology based on BP neural network, the image extraction technology based on GAN network and the image extraction technology based on CNN, the model based on GAN shows the best performance. This section also compares the performance of GAN with improved GAN algorithms, namely Dense-GAN and GA-GAN algorithms. The results verify that the improved model algorithm is better than the unimproved GAN model, and the performance of the two improved algorithms is not much different. Relatively speaking, the image reconstruction model based on the GA-GAN model has a better effect on the image reconstruction of the Tang Sancai figurines.

## 6. Conclusion

Blurred image restoration is an important branch of computer vision and image processing, which has important research and practical application value. Blurred image restoration based on deep learning is a research hotspot in recent years. An "end-to-end" image deblurring approach simplifies the solution of this problem. Although some GAN models based on convolutional networks are able to produce sharp and detailed images, it severely affects the learner's understanding of specific structures and features due to the limitation of the receptive field. In this paper, the global context module of geometric images is introduced into the global context modeling of input blurred images. By combining local contextual and global contextual information, it helps to generate clear images containing every detail. In this model, we also use the residual set structure to directly transmit low-frequency information through frequency hopping, which makes the network pay more attention to the learning of high-frequency information.

## Funding

This article is not supported by any foundation.

## Data Availability

Data sharing is not applicable to this article as no new data were created or analysed in this study.

## Conflict of Interest

The author states that this article has no conflict of interest.

## References

- [1] Zhang J, Zhang Y. *Design and Implementation of Edge Extraction Algorithm for Digital Image*. *International Core Journal of Engineering*. (2019) 5(9): 105-115.
- [2] Hu S. *Research on Data Acquisition Algorithms Based on Image Processing and Artificial Intelligence*. *International Journal of Pattern Recognition and Artificial Intelligence*. (2020) 34(06): 1-13. <https://doi.org/10.1142/S0218001420540166>
- [3] Ohanian T. *How Artificial Intelligence and Machine Learning May Eventually Change Content Creation Methodologies*. *SMPTE Motion Imaging Journal*. (2019) 128(1): 33-40. <https://doi.org/10.5594/JMI.2018.2876781>
- [4] Bhargavi V R, Rajesh V. *Computer Aided Bright Lesion Classification in Fundus Image Based on Feature Extraction*. *International Journal of Pattern Recognition and Artificial Intelligence*. (2018) 32(11): 1850034.1-1850034.15. <https://doi.org/10.1142/S0218001418500349>
- [5] Wang X, Xie Q, Ma T, et al. *Feature Extraction Based on Dimension Reduction and Clustering for Maize Leaf Spot Images*. *International Journal of Pattern Recognition & Artificial Intelligence*. (2018) 32(12): 1854029.1-1854029.15. <https://doi.org/10.1142/S0218001418540290>
- [6] Gupta H, Jin K H, Nguyen H Q, et al. *CNN-Based Projected Gradient Descent for Consistent Image Reconstruction*. *IEEE Transactions on Medical Imaging*. (2017) 37(6): 1-1. <https://doi.org/10.1109/TMI.2018.2832656>
- [7] Oliveira E, Gama J, Vale Z, et al. [Lecture Notes in Computer Science] *Progress in Artificial Intelligence Volume 10423 || Image Matching Algorithm Based on Hashes Extraction*. (2017) 10.1007/978-3-319-65340-2(Chapter 8): 87-94. [https://doi.org/10.1007/978-3-319-65340-2\\_8](https://doi.org/10.1007/978-3-319-65340-2_8)
- [8] Zhang X, Zhou J, Cherry S R, et al. *Quantitative image reconstruction for total-body PET imaging using the 2-meter long EXPLORER scanner*. *Physics in Medicine and Biology*. (2017) 62(6): 2465-2485. <https://doi.org/10.1088/1361-6560/aa5e46>
- [9] Yunjie Yang, Jiabin, et al. *A Miniature Electrical Impedance Tomography Sensor and 3-D Image Reconstruction for Cell Imaging*. *IEEE Sensors Journal*. (2017) 17(2): 514-523. <https://doi.org/10.1109/JSEN.2016.2631263>
- [10] Matthews T, Wang K, Li C, et al. *Regularized Dual Averaging Image Reconstruction for Full-Wave Ultrasound Computed Tomography*. *IEEE Transactions on Ultrasonics Ferroelectrics & Frequency Control*. (2017) 64(5): 811-825. <https://doi.org/10.1109/TUFFC.2017.2682061>
- [11] Yu H, Shan X, Wang S, et al. *Achieving High Spatial Resolution Surface Plasmon Resonance Microscopy with Image Reconstruction*. *Analytical Chemistry*. (2017) 89(5): 2704-2707. <https://doi.org/10.1021/acs.analchem.6b05049>
- [12] Ramon A J, Yang Y, Pretorius P H, et al. *Investigation of dose reduction in cardiac perfusion SPECT via optimization and choice of the image reconstruction strategy*. *Journal of Nuclear Cardiology*. (2017) 25(6): 1-12. <https://doi.org/10.1007/s12350-017-0920-1>
- [13] Ozan, ktem, Chong, et al. *Shape-based image reconstruction using linearized deformations*. *Inverse Problems*. (2017) 33(3): 1-1. <https://doi.org/10.1088/1361-6420/aa55af>
- [14] Ellis S, Reader A J. *Simultaneous maximum a posteriori longitudinal PET image reconstruction*. *Physics in Medicine and Biology*. (2017) 62(17): 6963-6979. <https://doi.org/10.1088/1361-6560/aa7b49>
- [15] Yin J, Yu W, Jia X. *Hybrid Norm Pursuit Method for Hyperspectral Image Reconstruction*. *IEEE Journal of Selected Topics in Applied Earth Observations and Remote Sensing*. (2017) 9(9): 1-9. <https://doi.org/10.1109/JSTARS.2016.2535467>

- [16] Zhang H, Wang L, Duan Y, et al. Euler's Elastica Strategy for Limited-Angle Computed Tomography Image Reconstruction. *IEEE Transactions on Nuclear Science*. (2017) 64(8): 2395-2405. <https://doi.org/10.1109/TNS.2017.2717864>
- [17] Lin Y, Shou K, Huang L. The initial study of LLS-based binocular stereo-vision system on underwater 3D image reconstruction in the laboratory. *Journal of Marine Science & Technology*. (2017) 22(3): 513-532. <https://doi.org/10.1007/s00773-017-0432-3>
- [18] Chen H Y, Ng L S, Chang C S, et al. Pursuing Mirror Image Reconstruction in Unilateral Microtia: Customizing Auricular Framework by Application of Three-Dimensional Imaging and Three-Dimensional Printing. *Plastic & Reconstructive Surgery*. (2017) 139(6): 1433-1443. <https://doi.org/10.1097/PRS.0000000000003374>
- [19] Guo Y, Li Z, Wang C, et al. Image reconstruction model for the exterior problem of computed tomography based on weighted directional total variation. *Applied Mathematical Modelling*. (2017) 52(dec.): 358-377. <https://doi.org/10.1016/j.apm.2017.07.057>
- [20] Balakin D A, Belinsky A V, Chirkin A S. Improvement of the optical image reconstruction based on multiplexed quantum ghost images. *Journal of Experimental & Theoretical Physics*. (2017) 125(2): 210-222. <https://doi.org/10.1134/S1063776117070147>